www.czasopisma.pan.pl PAN POLSKA AKADEMIA NAUK www.journals.pan.pl

Arch. Min. Sci. **64** (2019), 2, 279-296

Electronic version (in color) of this paper is available: http://mining.archives.pl

DOI 10.24425/ams.2019.128683

YUANYUAN PU*,**, DEREK B. APEL**#, YASHAR POURRAHIMIAN**, JIE CHEN*

EVALUATION OF ROCKBURST POTENTIAL IN KIMBERLITE USING FRUIT FLY OPTIMIZATION ALGORITHM AND GENERALIZED REGRESSION NEURAL NETWORKS

OCENA STANU ZAGROŻENIA TĄPANIA I WYRZUTÓW SKAŁ W KIMEBERLITE Z WYKORZYSTANIEM ALGORYTMU MUSZKI OWOCOWEJ I SIECI NEURONOWEJ REALIZUJĄCEJ UOGÓLNIONĄ REGRESJĘ (GRNN)

Rockburst is a common engineering geological hazard. In order to evaluate rockburst liability in kimberlite at an underground diamond mine, a method combining generalized regression neural networks (GRNN) and fruit fly optimization algorithm (FOA) is employed. Based on two fundamental premises of rockburst occurrence, depth, σ_θ, σ_c, σ_t, B_1, B_2, SCF, W_{et} are determined as indicators of rockburst, which are also input vectors of GRNN model. 132 groups of data obtained from rockburst cases from all over the world are chosen as training samples to train the GRNN model; FOA is used to seek the optimal parameter σ that generates the most accurate GRNN model. The trained GRNN model is adopted to evaluate burst liability in kimberlite pipes. The same eight rockburst indicators are acquired from lab tests, mine site and FEM model as test sample features. Evaluation results made by GRNN can be confirmed by a rockburst case at this mine. GRNN do not require any prior knowledge about the nature of the relationship between the input and output variables and avoid analyzing the mechanism of rockburst, which has a bright prospect for engineering rockburst potential evaluation.

Keywords: Rockburst potential evaluation, Generalized regression neural networks (GRNN), Fruit fly algorithm, Backpropagation neural network (BPNN)

Tąpnięcia skał są powszechnym i ogólnie znanym zagrożeniem dla środowiska geologicznego oraz dla budowli. Do oceny skłonności skał do tąpania w podziemnej kopalni diamentów w Kimberlite zastosowano metodę stanowiącą połączenie sieci neuronowych realizujących uogólnioną regresję i algorytm muszki owocowej. W oparciu o dwie podstawowe przesłanki wystąpienia tąpnięcia, głębokość oraz σ_θ, σ_c, σ_t, wielkości B_1, B_2, SCF, W_{et} określone zostały jako wskaźniki wystąpienia tąpnięcia i następnie wykorzystane jako wektory wejściowe w modelu sieci neuronowych GRNN. Zestawiono 132 zbiory danych o przypadkach tapnięć z całego świata i wykorzystano je jako zbiory uczące dla modelu sieci neuronowej realizującej uogólnioną regresję. Algorytm muszki owocowej wykorzystano do znalezienia optymalnej

* STATE KEY LABORARY OF COAL MINE DISASTER DYNAMICS AND CONTROL, CHONGQING UNIVERSITY, CHONGQING 400044, CHINA

** SCHOOL OF MINING AND PETROLEUM ENGINEERING, UNIVERSITY OF ALBERTA, EDMONTON, CANADA

Corresponding author: dapel@ualberta.ca

wartości parametru σ który umożliwi wygenerowanie najbardziej dokładnego modelu sieci neuronowej GRNN. Po treningu, model sieci GRNN wykorzystany został do oceny możliwości wystąpienia tąpnięcia w Kimberlite. Te same osiem wskaźników oceny skłonności wyrzutowej skały otrzymano na podstawie badań laboratoryjnych, z analiz prowadzonych w kopalni oraz w oparciu o metodę elementów skończonych, wyniki te wykorzystano następnie jako próbki danych. Wyniki uzyskane przy zastosowaniu sieci neuronowych realizujących regresję uogólnioną potwierdzone zostały przez wyniki uzyskane w trakcie wyrzutu w kopalni. Metoda sieci neuronowych nie wymaga uprzedniej wiedzy o naturze zależności pomiędzy zmiennymi wejściowymi i wyjściowymi i pozwala uniknąć analiz mechanizmu wyrzutu i tąpnięcia, co jest cechą pożądaną z punktu widzenia inżynierów odpowiedzialnych za ocenę skłonności skał do wyrzutu.

Słowa kluczowe: ocena możliwości wystąpienia wyrzutów skał, sieć neuronowa realizująca regresję uogólnioną (GRNN), algorytm muszki owocowej, sieć neuronowa realizującą propagację wsteczną (BPNN)

1. Introduction

Rockburst is a sudden geodynamic event that occurs in underground mines under stress impaction and, oftentimes, results in equipment damages and life injuries or even deaths (He et al., 2017; Mansurov, 2001). Most of mining countries have records of rockburst events, including China (Shi et al., 2005), Germany (Baltz & Hucke, 2008), Australia (Potvin et al., 2000), South Africa (Gibowicz, 2009), Canada (Blake & Hedley, 2003), Poland (Patyńska & Kabiesz, 2009; Bukowska 2012), United States (Iannacchione & Zelanko, 1993) et al. Due to serious consequence caused by rockburst, the rockburst potential evaluation is of great importance in the design stage, during construction and mining production (J. Zhou et al., 2012). Based on the analysis of different aspects of the rockburst mechanism, such as strength, stiffness, energy, stability, damage-fracture, many researchers were able to put forward some rockburst potential evaluation methods. For example, Kidybinski (Kidybiński, 1981) used strain energy storage index as a burst liability criterion. Mitri (Mitri et al., 2011) developed an energy-based burst potential index (BPI) to diagnose the burst proneness. Xie Heping (Xie & Pariseau, 1993) proposed a rockburst prediction method based on fractal dimension of rocks. However, influence factors of rockburst including mechanical condition, brittleness, energy-store condition, and mining or excavation methods, are complex. Furthermore, the relationships between rockburst intensity and these impact factors are highly non-linear, which makes the traditional, mechanism-based predication methods unable to create a precise evaluation for rockburst potential at underground mining. Hence, other researchers tried to analyze the relationship between rockburst control factors and rockburst intensity using some mathematical and statistical methods, such as fuzzy mathematics (W. Cai et al., 2016), neural network (Sun et al., 2009; Jia et al., 2013; Pu et al., 2018a; W. Gao, 2015), support vector machine (J. Zhou et al. 2012; Pu et al. 2018c) and decision tree (Pu et al., 2018b). These methods are more effective in processing non-linear problems, which train the model with existing data instead of discussing the rockburst mechanism.

A neural network is an important method in the area of artificial intelligence and is an excellent solution of coping with non-linear problems based on its strong self-learning ability. Neural networks do not need any prior knowledge about the nature of the relationship between the input/output variables, which is one of the benefits they have compared to most empirical and statistical methods. After Einstein (Dershowitz & Einstein, 1984) introduced artificial intelligence in rock mechanics in the 1980s, the neural network became widely used in rock and soil engineering (Ni et al., 1996; Nikbakhtan et al., 2015).

For rockburst potential evaluation, neural network has been an innovative approach based on its capability for operating non-linear relationship compared with traditional mechanism-based evaluation methods. Sun (Sun et al., 2009) combined fuzzy mathematics and a backpropagation neural network (BPNN) to evaluate rockburst liability in Sahelian coal mine. Dong (Dong et al., 2013) achieved rockburst liability evaluation results by comparing three optimization algorithms which implemented on a support vector machine (SVM). Zhou (K. Zhou & Gu, 2004) employed a self-organization neural network which was trained by data gained from a geographical information system (GIS) to assess burst liability at a deep metal mine. Zhang (Y. Zhang et al., 2017) built a rockburst pre-warning system with BPNN which fed by rock acoustic emission signals obtained from lab acoustic emission experiment. However, some defects were embedded into current researches. The performance of backpropagation neural network which were frequently used in current researches strongly relied on the determination of several hyper-parameters such as the number of layers, the study rate during gradient decent process. Researcher's experience would have a big impact on prediction results. Furthermore, the number of training samples in many researches were insufficient (most of them were less than 50). The lack of training sample easily resulted in overfitting which means neural network performs well only for training samples but awfully for real test samples. Neural network cannot operate on label data directly, which requires rockburst categories must be converted to a numerical form when fed into model. Most current researches simply converted categories with an integer. For example, if rockburst has four categories 'no', 'moderate', 'strong' and 'violent', '1', '2', '3', '4' were assigned to each category respectively. But a problem was raised that this method endowed a natural ordered relationship among categories. However, there is no this kind of relationship among rockburst categories.

In this paper, a novel generalized regression neural network (GRNN) was employed to build a relationship between rockburst levels and its indicators. A new optimization algorithm was employed to seek the unique parameter for GRNN. More than one hundred data collected from rockburst cases were used to train GRNN. Meanwhile, one-hot encoding was adopted to convert rockburst categories to numerical forms. Finally, this trained GRNN would be used to evaluate rockburst potential in two kimberlite pipes at a diamond mine.

2. Basic principle of GRNN

In general, frequently used neural networks include ordinary backpropagation neural network (BPNN), radial basis function neural network (RBFN), Hopfield neural network (HNN), recurrent neural network (RNN) and general regression neural network (GRNN). The core process of prediction with a neural network includes: choosing a suitable neural network, collecting training samples for the neural network, determining the input and output vectors based on the training sample, setting the parameters for the neural network, training the neural network, and prediction with the trained neural network. The key for neural network prediction lays in neural network selection and parameters (including hyper-parameters) setting. The less parameters subjectively determined by users, the more reliable the neural network is. The general regression neural network (GRNN has a fixed structure as long as the training samples are determined and only one subjective parameter is required which is suitable for prediction for engineering problems.

The GRNN is based on nonlinear regression theory (Specht, 1991). Compared to the traditional BPNN, the GRNN performs better at nonlinear mapping, and also, it can obtain more reasonable prediction results even if the training samples are inadequate (Cigizoglu & Alp,

2006). The GRNN has been successfully used to predict the load-bearing capacity of driven piles in cohesionless soils (Kiefa, 1998), estimate river suspended sediments (Cigizoglu & Alp, 2006), predict settlements (Sivakugan et al., 1998), analyze rock mechanics testing (Tutumluer & Seyhan, 1998), and solve other engineering problems.

GRNN is a variation radial basis neural network suggested by Specht (Specht, 1991). The x, y are both random variables, and $f(x,y)$ represents its joint probability density function. When we designate X as the observed value of x, the regression of y on X is given by:

$$\hat{Y} = E\left(y|X\right) = \frac{\int_{-\infty}^{\infty} y * f\left(X,y\right)dy}{\int_{-\infty}^{\infty} f\left(X,y\right)dy} \tag{1}$$

Assume $f(x,y)$ are normally distributed:

$$\hat{f}\left(\mathrm{X},\mathrm{Y}\right) = \frac{1}{n*\left(2\pi\right)^{\frac{d+1}{2}} * \sigma^{(d+1)}} \sum_{i=1}^{n} \exp\left[-\frac{\left(X-X_i\right)^T\left(X-X_i\right)}{2\sigma^2}\right] * \exp\left[-\frac{\left(Y-Y_i\right)^2}{2\sigma^2}\right] \tag{2}$$

In formula (2), n represents the number of training samples, d reflects the dimensions of the variable x (the number of features), σ represents a parameter called 'spread', which is the decisive factor GRNN. We use $\hat{f}(X,Y)$ to replace $f(x,y)$, and then, combine (1) and (2) to formula (3), where Y_i refers the output of the i^{th} training sample and X_i is the input feature vector of the i^{th} training sample.

$$\hat{Y} = \frac{\sum_{i=1}^{n} Y_i \exp\left[-\frac{\left(X-X_i\right)^T\left(X-X_i\right)}{2\sigma^2}\right]}{\sum_{i=1}^{n} \exp\left[-\frac{\left(X-X_i\right)^T\left(X-X_i\right)}{2\sigma^2}\right]} \tag{3}$$

We assume

$$P_i = \exp\left[-\frac{\left(X-X_i\right)^T\left(X-X_i\right)}{2\sigma^2}\right] \tag{5}$$

If

$$S_N = \sum_{i=1}^{n} Y_i P_i \tag{6}$$

$$S_D = \sum_{i=1}^{n} P_i \tag{7}$$

We have the final output of this GRNN $\hat{Y}$.

$$\hat{Y} = \frac{S_N}{S_D} \tag{8}$$

GRNN includes a four-layer network structure, consists of input layer, pattern layer, summation layer, and output layer. The number of neuros for input layer (first layer) is the amount of features of a training sample while numbers of neuros for pattern layer equal the number of training samples.

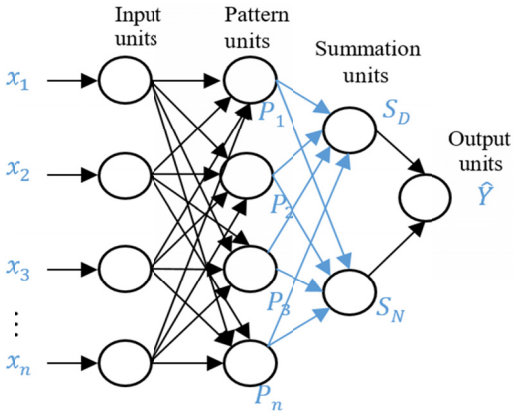

Fig. 1. GRNN block diagram

After pattern units receive information from input units, formula (5) will be used to convert this information, and then transport results into summation units. Formulas (6) and (7) are used in summation units. At last, formula (8) is employed to obtain the final output result (Jia et al., 2013). In GRNN, only one parameter, σ, needs to be set subjectively, which lowers the method's subjectivity compared to other neural network models. The key point of using GRNN in predicting an engineering problem is to determine a suitable σ.

3. The optimization of GRNN

In general, in order to determine σ, trial and error method is adopted, which usually results in a low efficiency and a weak precision. Actually, the most suitable σ is the one resulting in the lowest error between target and the output result of GRNN. Mathematically, the process of looking for a suitable σ can be regarded as a process of seeking a minimal value of this error. In this paper, a novel Fruit Fly Optimization Algorithm (FOA) is employed for seeking an optimal σ.

FOA was first applied to evaluate corporate performance in economics (Pan, 2011). According to simulations of a fruit fly's searching for food, the FOA can obtain the extreme value of a function. In the process of seeking an optimal σ for GRNN, the decision function is the error between the target and the prediction value, which means that this σ can result in a minimal value of the decision function. Here, the cross entropy (C.H. Li & Lee, 1993) was adopted to show the error between prediction values and targets. Minimizing cross entropy leads to good classifiers. Formula (9) demonstrates a cross entropy. Where y_i is the prediction result while y_i' is the target.

$$H_{y'}(y) = -\sum_i y_i' \log(y_i) \tag{9}$$

The MATLAB software (Manual 1995) helps us with performing this procedure. The steps are as follows:

Step 1: Determine the fruit flies' population size and the maximum number of iterations. Randomly initialize of the fruit flies' original location.

Step 2: Fruit flies start seeking food. Calculate the distance between the fruit fly individuals and the original point and calculate the decision value of flavor which is the reciprocal of this distance. This decision value of flavor is actually σ.

Step 3: The σ obtained in Step 2 is plugged into a GRNN training box in MATLAB (function statement: net = newgrnn (P,T,σ), where P and T represent input vector and output vector respectively). After GRNN training, function 'sim' will be used for simulation. The cross entropy between the simulation output vector and the targets will be represented as a decision function.

Step 4: The value of σ, which results in a minimum value of the decision function will be found out.

Step 5: Record this σ and corresponding coordinates (X, Y). At this time, the fruit fly population will fly to this location (X, Y).

Step 6: Iterative optimization. Step 2 to Step 4 will be executed repetitively. Every time, we will check if the obtained minimum value of the decision function is lower than the previous one. If yes, Step 5 will be executed. Figure 2 shows the flow of optimized GRNN using FOA.

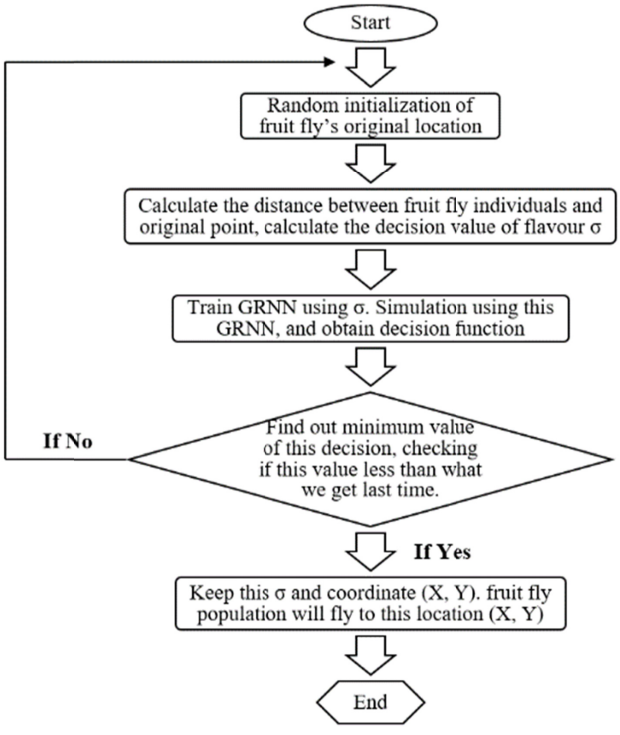

Fig. 2. The flow of optimized GRNN using FOA

4. Rockburst prediction with GRNN

The mechanism of rockburst is very complex and is influenced by many factors. Fundamentally, the rockburst occurrence has to meet two necessary requirements: the rock has to have the capability to accumulate strain energy and the environment should be favorable to stress concentration (M. Cai, 2016). Many single factor evaluation methods have been put forward aiming to estimate rockburst potential based on these two basic requirements. This includes the Cover Depth (D) (S.P. Singh, 1989), Strain Energy Storage Index (W_{et}) (Kidybiński, 1981), Stress Concentration Factor ($SCF = \sigma_\theta / \sigma_c$) (Martin et al. 1999), rock brittleness index $B_1 (B_1 = \sigma_c / \sigma_t)$ (Zhu et al. 1996), rock brittleness index $B_2 (B_2 = (\sigma_c - \sigma_t)/(\sigma_c + \sigma_t))$ (S. Singh 1987). Some indicators reflect the capability of stress storage while others represent stress concentration around underground excavations. In order to evaluate burst liability, the indicators which account for two basic requirements of rockburst occurrence should be combined. In this paper, eight indicators: depth (D), maximum shear stress around tunnel wall (σ_θ), uniaxial compressive strength (σ_c), uniaxial tensile stress (σ_t), rock brittleness index B_1, rock brittleness index B_2, Stress Concentration Factor (SCF), Strain Energy Storage Index (W_{et}) were working together to determine burst liability in kimberlite. These eight indicators constitute input features of a training sample for GRNN.

Most researchers divided rockburst activities into four levels (no rockburst, moderate rockburst, strong rockburst and violent rockburst) based on damage intensity, violence and scale (Russenes, 1974; Tan, 1992; Y. Wang et al., 1998). These four levels are labels (output vector) of GRNN. However, many machine learning algorithms including GRNN cannot operate using label data directly. They require all input variables and output variables to be numeric, which means the label data must be converted to a numerical form (Brownlee, 2018). Two ways can be adopted to convert the label data to a numerical form. The common method is the integer encoding which means each unique category is assigned an integer value. For example, we can assign '0' to 'no rockburst', '1' to 'moderate rockburst' and so on. However, integer encoding may result in poor performance or unexpected results because it assumes a natural ordering between categories when operating variables without such ordinal relationship such as rockburst levels. Alternatively, we can use one-hot encoding which means applying a binary variable for each category. In this case, 'no rockburst' can be encoded as [1 0 0 0]; 'moderate rockburst' can be encoded as [0 1 0 0] and so on.

In this study, 132 groups of data which came from rockburst cases from all over the world were chosen as training samples. Table 1 shows data where rockburst levels had been converted to one-hot encodings.

Data groups 1 to 100 are used as training samples while groups 101 to 132 are used as validation samples for parameter optimization. To avoid different units among eight features of training sample, data normalization was conducted to locate each feature in range [0,1]. Formula (10) was adopted to conduct normalization. Random initialization of fruit flies' location is in range [0,1]. After normalization, a typical training sample (case one) is like this: an eight-dimensional input vector (0.063 0.296 0.617 0.684 0.901 0.162 0.735 0.281) as well as the output vector (0 0 1 0). The fruit fly group consists of 20 individuals. The number of iteration is 100. Figure 3 shows optimization process and fruit flies' locations. After 100 iterations, the minimum value of error stabilizes at 0.679. The corresponding σ is 0.192.

$$x^* = \frac{x - x_{\min}}{x_{\max} - x_{\min}} \tag{10}$$

TABLE 1

Data set of training samples

Case number	Rock type	Depth/m	σ_θ/MPa	σ_c/MPa	σ_t/MPa	*SCF*	B_1	B_2	W_{et}	Burst Ranking	One-hot encoding	Data source
1	Granodiorite	200	90	170	11.3	0.53	15.04	0.88	9	STRONG	[0 0 1 0]	
2	Syenite	194	90	220	7.4	0.41	29.73	0.93	7.3	MODERATE	[0 1 0 0]	
3	Granodiorite	400	62.6	165	9.4	0.38	17.53	0.89	9	MODERATE	[0 1 0 0]	
4	Granite	300	55.4	176	7.3	0.32	24.11	0.92	9.3	STRONG	[0 0 1 0]	
5	Dolomitic Limestone	400	30	88.7	3.7	0.34	23.97	0.92	6.6	STRONG	[0 0 1 0]	
6	Granite	700	48.75	180	8.3	0.27	21.69	0.91	5	STRONG	[0 0 1 0]	
7	Quartzite	250	80	180	6.7	0.44	26.87	0.93	5.5	MODERATE	[0 1 0 0]	
8	Quartz Diorite	890	89	236	8.3	0.38	28.43	0.93	5	STRONG	[0 0 1 0]	
9	Marble	150	98.6	120	6.5	0.82	18.46	0.9	3.8	STRONG	[0 0 1 0]	(Y. Wang et al. 1998)
10	Biotite granite porphyry	203	91.23	157.63	11.96	0.58	13.18	0.86	6.27	VIOLENT	[0 0 0 1]	
11	Biotite granite porphyry	827	66.77	148.48	8.47	0.45	17.53	0.89	5.08	MODERATE	[0 1 0 0]	
12	Biotite granite porphyry	896	51.5	132.05	6.33	0.39	20.86	0.91	4.63	STRONG	[0 0 1 0]	
13	Biotite granite porphyry	1117	35.82	127.93	4.43	0.28	28.9	0.93	3.67	MODERATE	[0 1 0 0]	
14	Biotite limestone	1124	21.5	107.52	2.98	0.2	36.04	0.95	2.29	NONE	[1 0 0 0]	
15	Biotite limestone	1140	18.32	96.41	2.01	0.19	47.93	0.96	1.87	NONE	[1 0 0 0]	
16	Biotite limestone	983	110.3	167.19	12.67	0.66	13.2	0.86	6.83	VIOLENT	[0 0 0 1]	
17	Biotite limestone	853	26.06	118.46	3.51	0.22	33.75	0.94	2.89	MODERATE	[0 1 0 0]	(L. Zhang et al. 2010)
18	Biotite granite porphyry	644	16.62	156.86	10.66	0.11	14.71	0.87	4.83	STRONG	[0 0 1 0]	
19	Biotite granite porphyry	692	16.47	156.9	10.33	0.11	15.19	0.88	4.39	STRONG	[0 0 1 0]	
20	Biotite granite porphyry	970	16.43	157.95	11.06	0.1	14.28	0.87	4.99	VIOLENT	[0 0 0 1]	
21	Biotite granite porphyry	850	16.3	155.28	10.63	0.11	14.61	0.87	4.4	STRONG	[0 0 1 0]	(J. Zhang et al. 2011)
22	Biotite granite porphyry	174	15.97	114.07	11.96	0.14	9.54	0.81	2.4	NONE	[1 0 0 0]	
23	Biotite granite porphyry	275	19.14	106.31	11.96	0.18	8.89	0.8	2.07	NONE	[1 0 0 0]	
24	Biotite granite porphyry	187	12.96	117.81	11.96	0.11	9.85	0.82	2.49	NONE	[1 0 0 0]	
25	Biotite granite porphyry	267	31.05	147.85	11.96	0.21	12.36	0.85	3	STRONG	[0 0 1 0]	
26	Biotite granite porphyry	215	29.09	138.5	11.96	0.21	11.58	0.84	2.77	NONE	[1 0 0 0]	
27	Biotite granite porphyry	272	32.4	140.88	11.96	0.23	11.78	0.84	2.86	MODERATE	[0 1 0 0]	
28	Biotite granite porphyry	644	34.89	151.7	10.66	0.23	14.23	0.87	3.17	MODERATE	[0 1 0 0]	
29	Biotite granite porphyry	692	16.21	135.07	10.33	0.12	13.08	0.86	2.49	MODERATE	[0 1 0 0]	
30	Biotite granite porphyry	970	30.56	160.83	11.06	0.19	14.54	0.87	3.63	VIOLENT	[0 0 0 1]	

www.czasopisma.pan.pl PAN www.journals.pan.pl

31	Biotite granite porphyry	1107	19.36	113.87	4.43	0.17	25.7	0.93	2.38	MODERATE	[0 1 0 0]	
32	Biotite limestone	1205	33.15	106.94	2.98	0.31	35.89	0.95	2.15	STRONG	[0 0 1 0]	
33	Biotite limestone	1184	9.74	88.51	2.98	0.11	29.7	0.93	1.77	NONE	[1 0 0 0]	
34	Biotite limestone	1373	11.75	83.96	2.98	0.14	28.17	0.93	2.15	NONE	[1 0 0 0]	
35	Biotite limestone	1689	39.94	117.48	2.98	0.34	39.42	0.95	2.37	MODERATE	[0 1 0 0]	
36	Biotite limestone	1606	39.82	128.46	2.98	0.31	43.11	0.95	2.4	STRONG	[0 0 1 0]	
37	Biotite limestone	1220	46.22	140.07	2.01	0.33	69.69	0.97	3.29	MODERATE	[0 1 0 0]	
38	Biotite limestone	920	30.95	123.79	12.67	0.25	9.77	0.81	2.57	MODERATE	[0 1 0 0]	
39	Biotite limestone	785	40.99	186.3	12.67	0.22	14.7	0.87	4.1	STRONG	[0 0 1 0]	
40	Biotite limestone	772	20.82	122.47	12.67	0.17	9.67	0.81	2.81	MODERATE	[0 1 0 0]	
41	Biotite limestone	644	36.09	164.05	12.67	0.22	12.95	0.86	3.59	STRONG	[0 0 1 0]	(C. Zhang et al. 2011)
42	Sandstone	920	34.15	54.2	12.1	0.63	4.48	0.63	3.17	MODERATE	[0 1 0 0]	(Tang et al. 2003)
43	Granite	1000	60	135	15.04	0.44	8.98	0.8	4.86	MODERATE	[0 1 0 0]	
44	Marble	1000	60	66.49	9.72	0.9	6.84	0.74	2.15	MODERATE	[0 1 0 0]	
45	Migmatite	1000	60	106.38	11.2	0.56	9.5	0.81	6.11	MODERATE	[0 1 0 0]	
46	Peridotite	1000	60	86.03	7.14	0.7	12.05	0.85	2.85	MODERATE	[0 1 0 0]	
47	Lherzolite	1000	60	149.19	9.3	0.4	16.04	0.88	3.5	MODERATE	[0 1 0 0]	(Yi et al. 2010)
48	Amphibolite	1000	60	136.79	10.42	0.44	13.13	0.86	2.12	MODERATE	[0 1 0 0]	
49	Sandstone	750	63.8	110	4.5	0.58	24.4	0.92	6.31	STRONG	[0 0 1 0]	
50	Dolomite	750	2.6	20	3	0.13	6.67	0.74	1.39	NONE	[1 0 0 0]	
51	Phosphate rock	750	44.4	120	5	0.37	24	0.92	5.1	MODERATE	[0 1 0 0]	
52	Red Shale	750	13.5	30	2.67	0.45	11.2	0.84	2.03	MODERATE	[0 1 0 0]	
53	Sandstone	700	70.4	110	4.5	0.64	24.4	0.92	6.31	STRONG	[0 0 1 0]	
54	Dolomite	700	3.8	20	3	0.19	6.67	0.74	1.39	NONE	[1 0 0 0]	
55	Phosphate rock	700	57.6	120	5	0.48	24	0.92	5.1	STRONG	[0 0 1 0]	
56	Red Shale	700	19.5	30	2.67	0.65	11.2	0.84	2.03	STRONG	[0 0 1 0]	
57	Sandstone	600	81.4	110	4.5	0.74	24.4	0.92	6.31	VIOLENT	[0 0 0 1]	
58	Dolomite	600	4.6	20	3	0.23	6.67	0.74	1.39	NONE	[1 0 0 0]	
59	Phosphate rock	600	73.2	120	5	0.61	24	0.92	5.1	STRONG	[0 0 1 0]	
60	Red Shale	600	30	30	2.67	1	11.2	0.84	2.03	VIOLENT	[0 0 0 1]	(Yang et al. 2010)
61	Limestone	510	15.2	53.8	5.56	0.28	9.68	0.81	1.92	NONE	[1 0 0 0]	
62	Diorite	510	88.9	142	13.2	0.63	10.7	0.83	3.62	VIOLENT	[0 0 0 1]	
63	Iron ore	510	59.82	85.8	7.31	0.7	11.7	0.84	2.78	STRONG	[0 0 1 0]	
64	Skarn	510	32.3	67.4	6.7	0.48	10.1	0.82	1.1	NONE	[1 0 0 0]	(L. Zhang and Li 2009)
65	Dolomitic limestone	225	30.1	88.7	3.7	0.34	23.97	0.92	6.6	VIOLENT	[0 0 0 1]	

www.czasopisma.pan.pl PAN www.journals.pan.pl

66	Granite	375	18.8	171.5	6.3	0.11	27.22	0.93	7	NONE	[1 0 0 0]	
67	Limestone	435	34	149	5.9	0.23	25.25	0.92	7.6	MODERATE	[0 1 0 0]	
68	Clay sandstone	250	38.2	53	3.9	0.72	13.59	0.86	1.6	NONE	[1 0 0 0]	
69	Marble	100	11.3	90	4.8	0.13	18.75	0.9	3.6	NONE	[1 0 0 0]	
70	Limestone	300	92	263	10.7	0.35	24.58	0.92	8	MODERATE	[0 1 0 0]	
71	Diorite	330	62.4	235	9.5	0.27	24.74	0.92	9	VIOLENT	[0 0 0 1]	
72	Granite	223	43.4	136.5	7.2	0.32	18.96	0.9	5.6	VIOLENT	[0 0 0 1]	
73	Diastatite anorthose	425	11	105	4.9	0.1	21.43	0.91	4.7	NONE	[1 0 0 0]	(Feng and Wang 1994)
74	Marble	428	18.7	81.2	10.6	0.23	7.66	0.77	1.5	NONE	[1 0 0 0]	
75	Marble	510	23.6	82.8	11.2	0.29	7.39	0.76	1.5	NONE	[1 0 0 0]	
76	Granite Porphyry	460	28.6	123.6	11.5	0.23	10.75	0.83	2.5	NONE	[1 0 0 0]	
77	Granite Porphyry	580	72	120.5	14.9	0.6	8.09	0.78	2.5	NONE	[1 0 0 0]	
78	Diorite	460	29.8	132.2	7.8	0.23	16.95	0.89	4.6	NONE	[1 0 0 0]	
79	Diorite	530	44.6	130.5	11.09	0.34	11.77	0.84	4.6	NONE	[1 0 0 0]	
80	Diorite	569	66.1	135.2	10.9	0.49	12.4	0.85	4.6	MODERATE	[0 1 0 0]	
81	Diorite	650	99.4	129.5	11.3	0.77	11.46	0.84	4.6	MODERATE	[0 1 0 0]	
82	Dioritic Porphyrite	515	33.6	156.3	10.2	0.21	15.32	0.88	5.2	MODERATE	[0 1 0 0]	
83	Dioritic Porphyrite	650	109.5	155.8	11.77	0.7	13.24	0.86	5.2	STRONG	[0 0 1 0]	
84	Magnetite	520	26.9	92.6	9.52	0.29	9.73	0.81	3.7	MODERATE	[0 1 0 0]	
85	Magnetite	550	38.3	90.1	10.2	0.43	8.83	0.8	3.7	STRONG	[0 0 1 0]	
86	Magnetite	630	83.9	95.6	8.69	0.88	11	0.83	3.7	MODERATE	[0 1 0 0]	
87	Granite	560	55.9	126.8	6.56	0.44	19.33	0.9	8.1	VIOLENT	[0 0 0 1]	
88	Granite	670	109.9	128.5	9.63	0.86	13.34	0.86	8.1	VIOLENT	[0 0 0 1]	
89	Skarn	570	59.9	96.5	8	0.62	12.06	0.85	1.8	MODERATE	[0 1 0 0]	
90	Quartzfeldspar Porphyry	600	68	106.8	6.1	0.64	17.51	0.89	7.2	VIOLENT	[0 0 0 1]	(Xu et al. 2008)
91	Limestone	682	50.6	63.83	5.06	0.79	12.61	0.85	2.23	MODERATE	[0 1 0 0]	
92	Limestone	682	50.6	85.36	4.91	0.59	17.38	0.89	3.41	MODERATE	[0 1 0 0]	
93	Lead-zinc	682	50.6	104.97	6.18	0.48	16.99	0.89	10.9	VIOLENT	[0 0 0 1]	
94	Pyrite	682	50.6	153.1	10.48	0.33	14.61	0.87	3.14	MODERATE	[0 1 0 0]	(S. L. Li 2000)
95	Gneissic granite	490	120.8	151.6	10.1	0.8	15.01	0.88	20	VIOLENT	[0 0 0 1]	
96	Porphyritic biotite granite	590	119.32	138.6	7.74	0.86	17.91	0.89	30	VIOLENT	[0 0 0 1]	
97	Porphyritic granite	595	95.67	127.37	10.51	0.75	12.12	0.85	30	VIOLENT	[0 0 0 1]	
98	Monzogranite	784	114.44	174.71	14.42	0.66	12.12	0.85	10	VIOLENT	[0 0 0 1]	

www.czasopisma.pan.pl PAN www.journals.pan.pl

99	Monzogranite	858	127.6	145.42	13.7	0.88	10.61	0.83	10	VIOLENT	[0 0 0 1]	
100	Monzogranite	951	126.41	158.03	14.32	0.8	11.04	0.83	10	VIOLENT	[0 0 0 1]	
101	Monzogranite	1170	108.53	113.37	10.43	0.96	10.87	0.83	10	VIOLENT	[0 0 0 1]	(J. Wang et al. 2009)
102	Metasandstone	240	29.04	124.15	5	0.23	24.83	0.92	4.39	NONE	[1 0 0 0]	
103	Sandy slate	437	40.87	139	6	0.29	23.17	0.92	0.81	NONE	[1 0 0 0]	
104	Metasandstone	490	50.09	124	5	0.4	24.8	0.92	6.53	MODERATE	[0 1 0 0]	
105	Sandy slate	720	59.09	88.25	3.6	0.67	24.51	0.92	6.14	STRONG	[0 0 1 0]	
106	Metasandstone	620	62.13	124	5	0.5	24.8	0.92	4.62	MODERATE	[0 1 0 0]	
107	Sandy slate	470	40.9	88.25	3.6	0.46	24.51	0.92	4.61	MODERATE	[0 1 0 0]	
108	Sandy slate	220	22.93	88.25	3.6	0.26	24.51	0.92	0.81	NONE	[1 0 0 0]	(Z. Zhang 2002)
109	Amphibolite plagiogneiss	720	47.5	86.3	15.6	0.55	5.53	0.69	6.3	STRONG	[0 0 1 0]	
110	Black mica oblique gneiss	720	47.5	61.1	5.3	0.78	11.53	0.84	7.2	STRONG	[0 0 1 0]	
111	Copper ore	720	47.5	99.2	7.3	0.48	13.59	0.86	8.31	STRONG	[0 0 1 0]	
112	Diabase	720	47.5	91.3	14.5	0.52	6.3	0.73	21	STRONG	[0 0 1 0]	
113	Amphibolite plagiogneiss	780	67.2	86.3	15.6	0.78	5.53	0.69	6.3	STRONG	[0 0 1 0]	
114	Black mica oblique gneiss	780	67.2	61.1	5.3	1.1	11.53	0.84	7.2	STRONG	[0 0 1 0]	
115	Copper ore	780	67.2	99.2	7.3	0.68	13.59	0.86	8.31	STRONG	[0 0 1 0]	
116	Diabase	780	67.2	91.3	14.5	0.74	6.3	0.73	21	STRONG	[0 0 1 0]	
117	Amphibolite plagiogneiss	840	77	86.3	15.6	0.89	5.53	0.69	6.3	VIOLENT	[0 0 0 1]	
118	Black mica oblique gneiss	840	77	61.1	5.3	1.26	11.53	0.84	7.2	VIOLENT	[0 0 0 1]	
119	Copper ore	840	77	99.2	7.3	0.78	13.59	0.86	8.31	VIOLENT	[0 0 0 1]	
120	Diabase	840	77	91.3	14.5	0.84	6.3	0.73	21	VIOLENT	[0 0 0 1]	
121	Amphibolite plagiogneiss	900	225.5	86.3	15.6	2.61	5.53	0.69	6.3	VIOLENT	[0 0 0 1]	
122	Black mica oblique gneiss	900	225.5	61.1	5.3	3.69	11.53	0.84	7.2	VIOLENT	[0 0 0 1]	
123	Copper ore	900	225.5	99.2	7.3	2.27	13.59	0.86	8.31	VIOLENT	[0 0 0 1]	
124	Diabase	900	225.5	91.3	14.5	2.47	6.3	0.73	21	VIOLENT	[0 0 0 1]	
125	Amphibolite plagiogneiss	960	274.3	86.3	15.6	3.18	5.53	0.69	6.3	VIOLENT	[0 0 0 1]	
126	Black mica oblique gneiss	960	274.3	61.1	5.3	4.49	11.53	0.84	7.2	VIOLENT	[0 0 0 1]	
127	Copper ore	960	274.3	99.2	7.3	2.77	13.59	0.86	8.31	VIOLENT	[0 0 0 1]	
128	Diabase	960	274.3	91.3	14.5	3	6.3	0.73	21	VIOLENT	[0 0 0 1]	
129	Amphibolite plagiogneiss	1020	297.8	86.3	15.6	3.45	5.53	0.69	6.3	VIOLENT	[0 0 0 1]	
130	Black mica oblique gneiss	1020	297.8	61.1	5.3	4.87	11.53	0.84	7.2	VIOLENT	[0 0 0 1]	
131	Copper ore	1020	297.8	99.2	7.3	3	13.59	0.86	8.31	VIOLENT	[0 0 0 1]	
132	Diabase	1020	297.8	91.3	14.5	3.26	6.3	0.73	21	VIOLENT	[0 0 0 1]	(Liu 2011)

www.czasopisma.pan.pl PAN www.journals.pan.pl

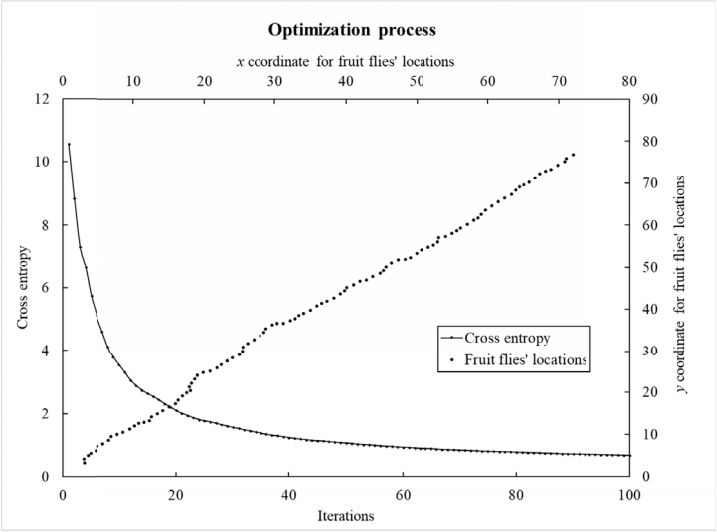

Fig. 3. The process of training GRNN with FOA

5. The rockburst prediction in kimberlite (at an underground diamond mine)

Kimberlite is the volcanic and volcanoclastic rock that sometimes bears diamonds. The analyzed case study comes from an underground diamond mine, located in northern, Canada., The statistical simulation of the rockburst potential of kimberlite was performed on samples obtained from two kimberlite pipes at this mine.

Fig. 4. View of typical open stope at the analyzed underground diamond mine (Photo by authors)

To determine the rockburst potential, twelve groups of kimberlite specimens from twelve different locations were collected from two pipes for rock mechanics test. Each group contains fifteen cylinder specimens which are divided into three sets with five specimens each. Three sets of specimens were used to do UCS test, uniaxial tensile test, and hysteresis loop test respectively (Leveille et al., 2016). When each rock specimen was collected, the in-situ stresses at each rock collection location were estimated. This was done by extracting the in-situ stresses data from a full-scale FEM model built at University of Alberta from data supplied by the mine. This model can be used for prediction of the mining induced stresses around underground excavations (Sepehri et al., 2017). Figure 5 shows the UCS test for a kimberlite sample and the in-situ stresses (σ_θ) extracting from an ABAQUS model. Table 2 shows the original data, which is adopted as the prediction sample.

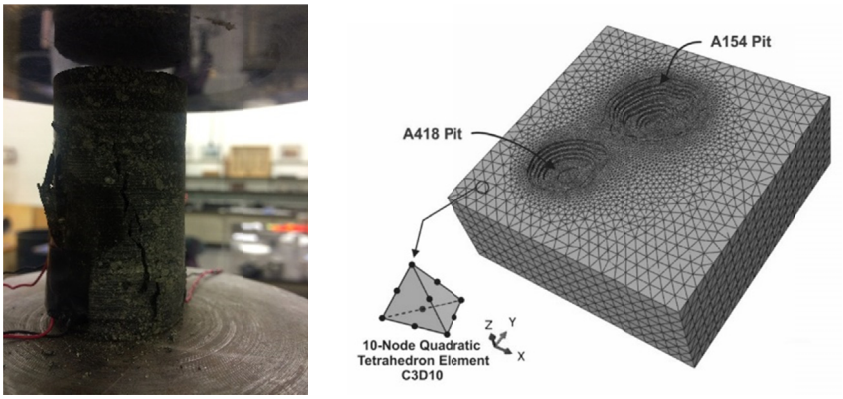

Fig. 5. The UCS test and the full-scale Abaqus model used for stresses extraction

TABLE 2

Features of test sample

Location	Depth/m	σ_0/MPa	σ_c/MPa	σ_t/MPa	*SCF*	B_1	B_2	W_{et}
1	226	18.17	49.10	1.56	0.37	31.40	0.94	3.30
2	226	21.00	60.00	3.17	0.35	18.90	0.90	1.70
3	226	31.16	82.00	3.87	0.38	21.20	0.91	2.30
4	300	46.38	74.80	2.98	0.62	25.10	0.92	3.20
5	300	48.64	76.00	4.09	0.64	18.60	0.90	2.50
6	300	22.92	57.30	1.43	0.40	40.00	0.95	1.50
7	413	99.09	112.60	3.74	0.88	30.10	0.94	5.20
8	413	35.16	79.90	3.12	0.44	25.60	0.92	2.50
9	413	15.84	49.50	2.16	0.32	22.90	0.92	2.80
10	550	13.02	65.10	2.28	0.20	28.50	0.93	1.20
11	550	21.12	52.80	2.18	0.40	24.20	0.92	2.30
12	550	29.12	57.10	3.34	0.51	17.10	0.89	2.20

The optimized GRNN is used to evaluate rockburst liability, and the evaluation results are as follows:

TABLE 3

Rockburst liability prediction results with GRNN

Group	Output vector	Rockburst prediction ranking
1	[0 1 0 0]	Moderate
2	[0 0 1 0]	Strong
3	[0 0 1 0]	Strong
4	[0 1 0 0]	Moderate
5	[0 1 0 0]	Moderate
6	[0 1 0 0]	Moderate
7	[0 1 0 0]	Moderate
8	[0 0 0 1]	Violent
9	[0 1 0 0]	Moderate
10	[0 1 0 0]	Moderate
11	[0 1 0 0]	Moderate
12	[0 1 0 0]	Moderate

Based on the GRNN evaluation, nine locations show 'moderate' burst liability, while two locations show 'strong' burst liability. The remaining one location have 'violent' burst liability. At least three cases of brittle and surficial failure occurred at the mine and were attributed to localized high stress accumulation and were classified as strain bursts (RioTinto, 2015). Figure 6 is a photo took at the mine (to be specific, at location 4). We can assert the ranking of this rockburst is moderate based on the observed phenomenon. However, at this stage of the mine development, the data on occurrence of rockburst is still limited and it would be difficult to make a claim that the proposed method can accurately depict kimberlite burst proneness at the mine.

Fig. 6. A rockburst case at diamond mine

Furthermore, a 3-layer ordinary (one hidden layer) backpropagation neural network (BPNN) is adopted to do the same job as a comparison. Table 1 is still used as training samples, while Table 2 is used as a test samples. For each group of data, there are the same eight indicators with GRNN which means the node number in input layer of BPNN is eight. The output layer node number is 4, because there are four rockburst rankings (none, moderate, strong, violent). An empirical formula (9) can be used to determine node number in the hidden layer (D. Gao, 1998). *S* represents node number in the hidden layer, while *m*, *n* reflect node number in input and output layers respectively. From formula (9), node number in the hidden layer is seven. The training goal is 0.001. The original training samples are normalized before feeding into BPNN. Table 4 shows the evaluation results with BPNN.

$$S = \sqrt{0.43mn + 0.12n^2 + 2.54m + 0.77n + 0.35} + 0.51 \tag{9}$$

TABLE 4

Rockburst liability prediction results with BPNN

Group	Output vector	Rockburst prediction ranking
1	[0.19 0.58 0.07 0.16]	Moderate
2	[0.37 0.36 0.11 0.22]	Cannot distinguish
3	[1.32 0.05 –0.62 –0.50]*	*Result out of scope**
4	[0.13 0.62 0.15 0.10]	Moderate
5	[0.36 –0.32 1.51 –0.11]*	*Result out of scope**
6	[0.68 1.96 0.72 –0.64]*	*Result out of scope**
7	[0 0.68 0.25 0.07]	Moderate
8	[0.88 0.11 0.01 0]	None
9	[0.74 0.17 0.09 0]	None
10	[0.25 –0.32 –0.55 –0.43]*	*Result out of scope**
11	[1.02 1.02 –0.46 –0.25]*	*Result out of scope**
12	[0 0.99 0.01 0]	Moderate

Based on the results summarized in Table 4, the BPNN cannot give an answer to each scenario. Only 6 groups show relatively clear results (group 1, 4, 7, 8, 9, 12), while 5 groups have out-of-scope prediction results. The remaining 1 group lacks confidence in distinguishing the rockburst severity, which tells us that we cannot evaluate rockburst ranking with this output vector. The primary cause of BPNN's poor performance mainly lays in the deficiency of the training sample (only 132 groups of training samples were provided). Hence, under the condition of the limited data we had, the GRNN was a better choice for our case study.

6. Conclusion

The general regression neural network method is used to evaluate burst liability in kimberlite, which avoids analyzing a complex mechanism of rockburst. The GRNN is based on the data alone to determine the structure and parameters of the model. A novel FOA method is adopted to optimize GRNN, which helps to determine the unique subjective parameter σ in GRNN model.

The FOA method reduces the randomness and subjectivity in choosing parameter, which increases the reliability of GRNN.

Eight indicators: depth, σ_θ, σ_c, σ_t, B_1, B_2, SCF, W_{et} are chosen as the input features of GRNN. These indicators combine two fundamental conditions for rockburst occurrence: the energy condition and rock mechanical condition, which result comprehensively in rockburst. Based on these eight indicators, GRNN can be used successfully as a solution to evaluate rockburst potential in different locations.

The evaluation result of GRNN exhibits a 'moderate' burst liability, which matches practical rockburst situations at the investigated mine (RioTinto, 2015). However, when the BPNN is adopted to predict, a poor result is showing. Compared to BPNN, GRNN is slightly affected by parameter setting, and also, is well-adapted for limited training samples. This FOA-GRNN method provides a new way for rockburst potential evaluation.

Acknowledgement

This study was supported by the Natural Sciences and Engineering Research Council of Canada (NSERC) under Collaborative Research and Development (CRD) Grant.

References

Baltz R., Hucke A., 2008. *Rockburst prevention in the German coal industry*. In Proceedings of the 27th international conference on ground control in mining. West Virginia University, Morgantown, WV, 46-50.

Blake W., Hedley D.G., 2003. *Rockbursts: case studies from North American hard-rock mines*: SME.

Brownlee J., 2018. *Why One-Hot Encode Data in Machine Learning*. Dostopno na: https://machinelearningmastery.com/why-one-hot-encode-data-in-machine-learning/, ogled.

Bukowska M., 2012. *The rockbursts in the upper silesian coal basin in Poland.* Journal of Mining Science **48** (3), 445-456.

Cai M., 2016. *Prediction and prevention of rockburst in metal mines – A case study of Sanshandao gold mine.* Journal of Rock Mechanics and Geotechnical Engineering **8** (2), 204-211, doi:10.1016/j.jrmge.2015.11.002.

Cai W., Dou L., Si G., Cao A., He J., Liu S., 2016. *A principal component analysis/fuzzy comprehensive evaluation model for coal burst liability assessment.* International Journal of Rock Mechanics and Mining Sciences **81**, 62-69.

Cigizoglu H.K., Alp M., 2006. *Generalized regression neural network in modelling river sediment yield.* Advances in Engineering Software **37** (2), 63-68.

Dershowitz W.S., Einstein H.H., 1984. *Application of artificial intelligence to problems of rock mechanics*. In The 25th US Symposium on Rock Mechanics (USRMS), American Rock Mechanics Association.

Dong L., Li X., Peng K. 2013. *Prediction of rockburst classification using Random Forest*. Transactions of Nonferrous Metals Society of China **23** (2), 472-477.

Feng X., Wang L., 1994. *Rockburst prediction based on neural networks.* Transactions of Nonferrous Metals Society of China **4** (1), 7-14.

Gao D., 1998. *On Structure of Supervised Linear Basis Function Feedforward Three-Layered Neural Networks (in Chinese).* Chinese J. Computer **21** (1), 80-86.

Gao W., 2015. *Forecasting of rockbursts in deep underground engineering based on abstraction ant colony clustering algorithm*. Natural Hazard **76** (3), 1625-1649.

Gibowicz S.J., 2009. *Seismicity induced by mining: Recent research.* Advances in Geophysics **51**, 1-53.

He J., Dou L., Gong S., Li J., Ma Z., 2017. *Rock burst assessment and prediction by dynamic and static stress analysis based on micro-seismic monitoring.* International Journal of Rock Mechanics and Mining Sciences **93**, 46-53.

Iannacchione A.T., Zelanko J.C., 1993. *Occurrence and remediation of coal mine bumps: a historical review*.

Jia Y., Lv Q., Shang Y., 2013. *Rockburst Prediction Using Particle Swarm Optimization Algorithm and General Regression Neural Network (in Chinese)*. Chinese Journal of Rock Mechanics and Engineering **32** (2), 343-348.

Kidybiński A., 1981. *Bursting liability indices of coal*. In International Journal of Rock Mechanics and Mining Sciences & Geomechanics Abstracts **18**, 295-304.

Kiefa M.A., 1998. *General regression neural networks for driven piles in cohesionless soils.* Journal of Geotechnical and Geoenvironmental Engineering **124** (12), 1177-1185.

Leveille P., Sepehri M., Apel D.B., 2016. *Rockburst Potential of Kimberlite: A Case Study of Diavik Diamond Mine.* Rock Mechanics and Rock Engineering, 1-9.

Li C.H., Lee C., 1993. *Minimum cross entropy thresholding*. Pattern Recognition **26** (4), 617-625.

Li S.L., 2000. *Study on rockburst proneness and strata control technology for deep mines with hard rock*. Ph.D Thesis, Northeastern University, Shengyang, China.

Liu J., 2011. *Studies on relationship between Microseism time-space evolution and ground pressure activities in deep mine*. Ph.D's Thesis, Northeastern University, Shengyang, China.

Mansurov V., 2001. *Prediction of rockbursts by analysis of induced seismicity data.* International Journal of Rock Mechanics and Mining Sciences **38** (6), 893-901.

Manual M., 1995. *the MathWorks.* Inc., Natick, MA.

Martin C., Kaiser P., McCreath D., 1999. *Hoek-Brown parameters for predicting the depth of brittle failure around tunnels.* Canadian Geotechnical Journal **36** (1), 136-151.

Mitri H.S., Hughes R., Zhang Y., 2011. *New rock stress factor for the stability graph method.* International Journal of Rock Mechanics and Mining Sciences **48** (1), 141-145.

Ni S., Lu P., Juang C., 1996. *A fuzzy neural network approach to evaluation of slope failure potential.* Computer-Aided Civil and Infrastructure Engineering **11 (**1), 59-66.

Nikbakhtan B., Apel D., Ahangari K. 2015. *Jet grouting: Using artificial neural networks to predict soilcrete column diameter K Part II. [Article]*. International Journal of Mining and Mineral Engineering **6** (1), 57-71, doi:10.1504/IJMME.2015.067951.

Pan W., 2011. *Using Fruit Fly Optimization Algorithm Optimized General Regression Neural Network to Construct the Operating Performance of Enterprises Model*. Journal of Taiyuan University of Technology (Social Sciences Edition) (in Chinese) **29** (4), 1-5.

Patyńska R., Kabiesz J., 2009. S*cale of seismic and rock burst hazard in the Silesian companies in Poland.* Mining Science and Technology (China) **19** (5), 604-608.

Potvin Y., Hudyma M., Jewell R.J., 2000. *Rockburst and seismic activity in underground Australian mines-an introduction to a new research project.* In ISRM International Symposium, International Society for Rock Mechanics.

Pu Y., Apel D., Xu H., 2018a. *A Principal Component Analysis/Fuzzy Comprehensive Evaluation for Rockburst Potential in Kimberlite*. Pure and Applied Geophysics, 1-11.

Pu Y., Apel D.B., Lingga B., 2018b. *Rockburst prediction in kimberlite using decision tree with incomplete data*. Journal of Sustainable Mining.

Pu Y., Apel D.B., Wang C., Wilson B., 2018c. *Evaluation of burst liability in kimberlite using support vector machine.* Acta Geophysica, 1-10.

RioTinto, 2015. *Serious potential incident review: Fall of Ground* (pp. 35). Yellownife, Canada: Rio Tinto.

Russenes B., 1974. *Analysis of rock spalling for tunnels in steep valley sides. Norwegian Institute of Technology,* Deptartment of Geology, Trondheim Google Scholar.

Sepehri M., Apel D., Liu W., 2017. *Stope Stability Assessment and Effect of Horizontal to Vertical Stress Ratio on the Yielding and Relaxation Zones Around Underground Open Stopes Using Empirical and Finite Element Methods.* Archives of Mining Sciences **62** (3), 653-669.

Shi Q., Pan Y., Li Y., 2005. *The Typical Cases and Analysis of Rockburst in China* (in Chinese). Coal Mining Technology **10** (2), 13-17.

Singh S. 1987. *The influence of rock properties on the occurrence and control of rockbursts.* Mining Science and Technology **5** (1), 11-18.

Singh S.P., 1989. *Classification of mine workings according to their rockburst proneness.* Mining Science and Technology **8** (3), 253-262.

Sivakugan N., Eckersley J., Li H., 1998. *Settlement predictions using neural networks.* Australian Civil Engineering Transactions **40**, 49.

Specht D.F., 1991. *A general regression neural network.* IEEE Transactions on Neural Network**s 2** (6), 568-576.

Sun J., Wang L., Zhang H., Shen Y., 2009. *Application of fuzzy neural network in predicting the risk of rock burst.* Procedia Earth and Planetary Science **1** (1), 536-543.

Tan Y., 1992. *Rockburst characteristics and structural effects of rock mass.* Science in China Series B-Chemistry, Life Sciences & Earth Sciences **35** (8), 981-990.

Tang S., Wu Z., Chen, X., 2003. *Approach to occurrence and mechanism of rockburst in deep underground mines* [J]. Chinese Journal of Rock Mechanics and Engineering **8**, 004.

Tutumluer E., Seyhan U., 1998. *Neural network modeling of anisotropic aggregate behavior from repeated load triaxial tests.* Transportation Research Record: Journal of the Transportation Research Board (1615), 86-93.

Wang J., Chen J., Yang J., Que J., 2009. *Method of distance discriminant analysis for determination of classification of rockburst.* Rock and Soil Mechanics **30** (7), 2203-2208.

Wang Y., Li W., Li Q., Xu Y., Tan G., 1998. *Method of fuzzy comprehensive evaluations for rockburst prediction.* Chinese Journal of Rock Mechanics and Engineerin **17** (5), 493-501.

Xie H., PariseauW.G., 1993. *Fractal character and mechanism of rock bursts*. In International Journal of Rock Mechanics and Mining Sciences & Geomechanics Abstracts **30**, 343-350, **4**: Elsevier

Xu M., Du Z., Yao G., Liu Z., 2008. *Rockburst prediction of chengchao iron mine during deep mining.* Chinese Journal of Rock Mechanics and Engineering **27** (s1), 2921-2928.

Yang J., Li X., Zhou Z., Lin Y., 2010. *A Fuzzy assessment method of rock-burst prediction based on rough set theory*. Jinshu Kuangshan/Metal Mine (**6**), 26-29.

Yi Y., Cao P., Pu C., 2010. *Multi-factorial Comprehensive Estimation for Jinchuan's Deep Typical Rockburst Tendency.* Keji Daobao/ Science & Technology Review **28** (2), 76-80.

Zhang C., Zhou H., Feng X.-T., 2011. *An index for estimating the stability of brittle surrounding rock mass: FAI and its engineering application.* Rock Mechanics and Rock Engineering **44** (4), 401.

Zhang J., Fu B., Li Z., Song S., Shang Y., 2011. *Criterion and classification for strain mode rockbursts based on five-factor comprehensive method*. In 12th ISRM Congress, International Society for Rock Mechanics.

Zhang L., Li C., 2009. *Study on tendency analysis of rockburst and comprehensive prediction of different types of surrounding rock*. In*, ……*

Zhang Y., Yang Z., Yao X., Liang P., Tian B., Sun L., 2017. *Experimental study of rockburst early warning method based on acoustic emission cluster analysis and neural network identification.* Rock and Soil Mechanics **38** (S2), 89-98.

Zhang Z., 2002. *Study on rockburst and large deformation of Xuefeng mountain tunnel of Shaohuai highway.* Master's Thesis, Chengdu University of Technology, Chengdu, China.

Zhou J., Li X., Shi X., 2012. *Long-term prediction model of rockburst in underground openings using heuristic algorithms and support vector machines.* Safety Science **50** (4), 629-644.

Zhou K., Gu D., 2004. *Application of GIS-based neural network with fuzzy self-organization to assessment of rockburst tendency*. Chinese Journal of Rock Mechanics and Engineering **23** (18), 3093-3097.

Zhu P., Wang Y., Li T., 1996. *Griffith theory and the criteria of rock burst.* Chinese Journal of Rock Mechanics and Engineering **15** (S1), 491-495.